Nuclear Engineering and Technology 55 (2023) 2604–2612

Contents lists available at ScienceDirect

Nuclear Engineering and Technology

journal homepage: www.elsevier.com/locate/net

Original Article

Modelling of the fire impact on CONSTOR RBMK-1500 cask thermal behavior in the open interim storage site

Robertas Poškas [a, *], Kęstutis Račkaitis [a], Povilas Poškas [a], Hussam Jouhara [b]

[a] Nuclear Engineering Laboratory, Lithuanian Energy Institute, Breslaujos 3, LT-44403, Kaunas, Lithuania
[b] Heat Pipe and Thermal Management Research Group, College of Engineering, Design and Physical Sciences, Brunel University London, Uxbridge, UB8 3PH, UK

ARTICLE INFO

Article history:
Received 1 April 2022
Received in revised form
5 January 2023
Accepted 16 April 2023
Available online 18 April 2023

Keywords:
RBMK-1500 spent nuclear fuel
Interim storage
Metal-concrete CONSTOR cask
Thermal analysis
Fire conditions

ABSTRACT

Spent nuclear fuel and long-lived radioactive waste must be carefully handled before disposing them off to a geological repository. After the pre-storage period in water pools, spent nuclear fuel is stored in casks, which are widely used for interim storage. Interim storage in casks is very important part in the whole cycle of nuclear energy generation. This paper presents the results of the numerical study that was performed to evaluate the thermal behavior of a metal-concrete CONSTOR RBMK−1500 cask loaded with spent nuclear fuel and placed in an open type interim storage facility which is under fire conditions (steady-state, fire, post-fire). The modelling was performed using the ANSYS Fluent code. Also, a local sensitivity analysis of thermal parameters on temperature variation was performed. The analysis demonstrated that the maximum increase in the fuel load temperatures is about 10 °C and 8 °C for 30 min 800 °C and 60 min 600 °C fires respectively. Therefore, during the fire and the post-fire periods, the fuel load temperatures did not exceed the 300°C limiting temperature set for an RBMK SNF cladding for long-term storage. This ensures that fire accident does not cause overheating of fuel rods in a cask.

1. Introduction

Spent nuclear fuel (SNF) and radioactive waste accumulated during the operation of a nuclear power plant should be properly managed during each step of their life cycle. However, the proper management of these wastes is a complex issue.

In a worldwide experience, disposal of long-lived radioactive waste and SNF (after recycling or not) in a geological repository is recognized as the final step of management. Before that final step, however, SNF should have been properly stored. The time of storage is determined based on SNF decay heat and radioactivity properties.

SNF assemblies are highly radioactive and emit a lot of heat, and therefore, after retrieval from the reactor core, they must be stored in special water pools (usually located at the reactor site). Water efficiently disperses heat from SNF and also acts as a barrier against radiation. SNF is kept in water pools for at least 5 years until the heat and radioactivity emission reduce. After this stage of storage, dry storage is widely applied. In interim storage, casks with inert gas or air are used to ensure spent fuel cooling under different conditions [1,2]. This technology is safe as it does not depend on external power sources. Also, its management is cost-effective [3]. The intended exploitation time of such interim storage facilities is usually up to 50 years [4].

The said casks are stored in specially designed buildings with or without central cooling systems or in open sites. Humidity, outside temperature and wind are not important factors if casks are stored indoors. Open sites are called open storage facilities. In this case, atmospheric temperature, humidity, wind and solar insolation become important factors and should be considered in safety evaluation [5].

Dry storage casks are produced of either metal or reinforced concrete, the latter being more cost-effective [1,6]. Some casks are used not only for storage but also for transportation. Such casks must meet requirements of the International Atomic Energy Agency (IAEA) [7], i.e., must protect the environment and people against radiation exposure [8,9].

There are two types of SNF storage casks: ventilated and non-ventilated. A wide range of investigations is performed for ventilated casks under normal storage conditions [10–12].

Other researches [13–15] investigated non-ventilated casks.

* Corresponding author.
E-mail address: Robertas.Poskas@lei.lt (R. Poškas).

https://doi.org/10.1016/j.net.2023.04.026

Also, some publications [16,17] provide a thermal analysis of RBMK−1500 SNF in cast iron (CASTOR) and metal-concrete (CONSTOR) non-ventilated casks. Publications [18,19] provide a detailed analysis of thermal processes for small-scale model down to the fuel rods with the Fluent code. These works present the comparison of the porous media and effective thermal conductivity approximations for modeling of fuel assemblies.

It is very important to prevent accidents in nuclear objects [20,21]. Publications on the analysis of the thermal performance of SNF casks during extreme conditions like fire are rather limited [9]. discussed safety issues of a non-ventilated cask with SNF under normal storage conditions and in the case of an accident during transportation, e.g., an impact of a fire. The 3D modeling for steady-state and transient conditions was carried out using the ANSYS finite element code. The evaluation of the maximal fuel temperature inside the cask was performed. The numerical analysis showed no safety issues. The set limiting temperatures had not been exceeded by the maximal temperatures of the cask packaging, and thus it was concluded that the tested packaging system had appropriate integrity.

[22] analyses SNF on fire during transportation. A 2D model of the cask was used in the ANSYS code. The fire accident investigation was split into several steps. At first, the modeling was performed using normal steady-state conditions. Those results were used as initial conditions for the fire accident. In the next step, transient calculations were performed in order to evaluate the fire and up to 20 hours post−fire periods. The analysis demonstrated that the transportation cask's performance with no spent fuel cladding failure is guaranteed for at least 7 hours in the case of fire with the temperature of 816 °C.

In [23], a numerical investigation of a fire accident in the case of a non-ventilated transportation cask was performed. The modelling results revealed that in order to obtain realistic data, the modeling must take into account more than just the conductive melting of lead shielding. Only coupling with an accurate turbulent model could show the influence of high Rayleigh number convection in the cask.

[8]presented results of experimental investigations of an open pool fire with a one-sixth piece of a dual-purpose (storage & transportation) cask. This cask was mainly designed for PWR SNF assembly's transportation. The investigations revealed the changes in thermal characteristics of the neutron shielding and fins of the dual purpose non-ventilated cask under fire conditions. Also, a numerical simulation of the experiment was performed using the ANSYS Fluent code. It was shown that the modeled temperatures were higher than the measured ones.

[24]published results of an investigation in which fires of a nuclear waste overpack were modeled numerically. Two prototypes were also tested experimentally. The comparison of the modeled and experimental values showed matched results.

The paper [25] presented results of a numerical modeling of a 30 minute 800 °C fire and its impact on the thermal behavior of a cast iron non-ventilated CONSTOR RBMK−1500 cask. The casks that were modeled in the investigation are stored in an open type dry storage facility for SNF located at the Ignalina NPP site. The modeling was performed using the ANSYS Fluent code for steady-state, fire and post-fire conditions. It was demonstrated that the most significant increase in the temperature during the fire and the initial period of post-fire is in the cask with the cast iron body. The increase in the temperature of the spent fuel load was not significant.

The present paper analyses results of the numerical modeling of the fire impact on the thermal behavior of a metal-concrete non-ventilated CONSTOR RBMK−1500 cask. The modeled cask is placed at the Ignalina Nuclear Power Plant site, open-type dry storage facility. The ANSYS Fluent tool was used for the modeling. The first step was to determine the distribution of the initial steady-state temperature when the storage conditions are normal (i.e., there is no fire). The second step was to introduce fire conditions (transient conditions), i.e., the temperatures of 800 °C and 600 °C and the durations of 30 minutes and 60 minutes, respectively. The third step was to perform an analysis of the post-fire cool down period (transient conditions).

2. Methodology

2.1. CONSTOR RBMK-1500 cask

This paper discusses heat removal from a metal-concrete CONSTOR RBMK−1500 non-ventilated cask, which is stored in an open interim storage facility at the Ignalina NPP site. It is surrounded by other storage casks. Only a solar insolation factor is taken into account for summer storage conditions. Other weather factors are less important for the analyzed case and were neglected.

The cask has a concrete cylinder body (1) steal lined from both sides (Fig. 1). The dimensions of such a cask are the following: the height is more than 4 m, the diameter is ~2 m, and the wall thickness is ~0.3 m. The stainless steel basket (5) is loaded with spent nuclear fuel bundles (fuel with 2% enrichment) and is placed into the cask [17]. The capacity of such a basket is 51 RBMK SNF assemblies that are cut in halves (102 fuel rod bundles) (13) with the burnup of 22.2 MWd/kg_{HM} and the cooling period of five years. Decay heat load produced by the 102 bundles is 7.14 kW [26]. The cask is firmly closed with a lid (10) and covered with a guard plate (8). The gaps between the basket and the cask body are filled with helium (4). The bottom helium gap (between the external side of the basket bottom and the internal side of the cask bottom) is about 10 mm thick, the vertical helium gap (between the sides of the basket and the cask) is about 10 mm thick and the top helium gap (between the upper part of the basket and cask lid) is about 30 mm thick. An air gap (9) (about 10 mm thick) is formed between the guard plate and the cask lid. The cask is stored in an open type facility on a concrete foundation and a reinforced concrete cover (7) is used for the covering of the cask.

The rather complex geometry of the cask and interacting processes of radiation, conduction and convection mean that the characterization of heat transfer processes is not a simple and easy task. Hence, the aim of thermal assessments of a spent nuclear fuel storage system is to ensure the reliability of the decay heat removal system applied. In other words, irrespective of the conditions—operational and accidental—the storage system components and the SNF must not reach greater temperature values than the limiting temperature values [27]. The proper SNF storage and the proper handling of the cask are indicated by the maximum allowable temperature of the claddings of the fuel rods and on the cask surface. The allowable temperature for the SNF rod claddings for long-term storage in a nitrogen or helium environment and in under conditions of normal operation is ~300 °C [28,29]. In the case of a fire, the elements inside the cask are affected thermally because of the radiative and convective fluxes influencing the temperature on the outer cask surface [22]. If an accident lasts for a short period of time, the temperature in the fuel load zone should stay lower than 570 °C [30].

2.2. Numerical modeling

In the case of normal operating conditions, heat is removed from the outer cask surface to the surroundings by thermal radiation and buoyancy-induced air flow, and in the case of fire, the situation is the opposite, i.e., heat approaches the outer cask surface from the

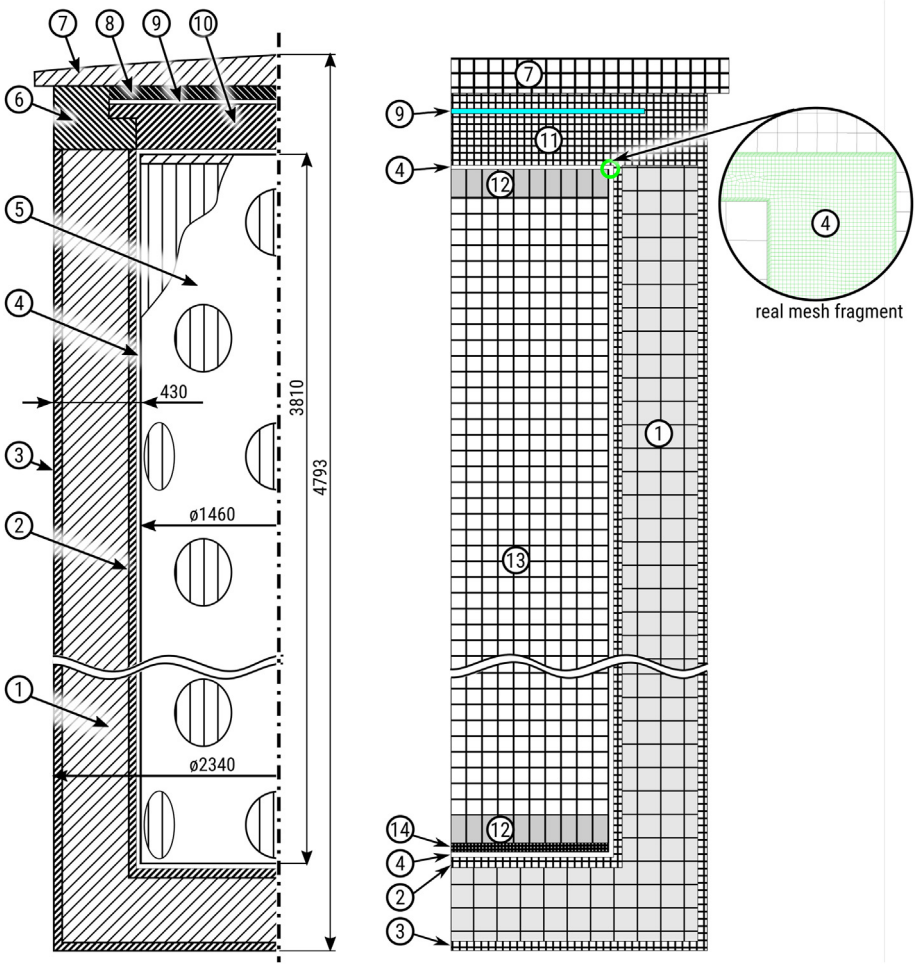

Fig. 1. Schemes of the cask and of the computer model (not to scale): 1 – cask body, 2 – inner lining, 3 – outer lining, 4 – helium gap, 5 – basket, 6 – cask top 7 – concrete cover, 8 – guard plate, 9 – air gap, 10 – cask lid, 11 – cask top, cask lid, guarding plate, 12 – not active zone, 13 – fuel load zone, 14 - basket bottom.

environment. The heat is transferred through the cylindrical wall of a storage cask by conduction, convection and radiation through helium and air gaps (Fig. 2).

Some studies perform homogenization of the fuel load area in order to make calculations simpler when the effective conductivity approach is applied in modeling [11,22,27]. The modelling described in the present paper also applied the effective axial coefficient and the radial heat conductivity coefficient for the assessment of heat transferring through fuel load. The said coefficients and other thermal properties of cask components are taken from the technical design. Helium thermal properties are taken from [31]. Variation of thermal properties with temperature is taken into account.

Probably the most crucial thermal impact on SNF casks is from maximum solar insolation during the longest day of summer. However, this impact is significantly decreased by the massive cask body. This paper presents the results of the modeling of a cask which is in an open storage facility in summer time under steady-state conditions and is exposed to solar irradiation while the temperature of the ambient air is 37 °C. The temperature value of the ambient air was calculated from the average summer temperature in Lithuania plus 10 °C to match the impact from the surrounding casks. The modeling employed a conservative approach, thus no decrease in temperature at night was considered. According to the IAEA [7], the vertical surface of the cask (the cylinder) is exposed to 200 W/m^2 and the horizontal surface (concrete cover) is exposed to 800 W/m^2 during a 12-hour period (daylight time). In this study, however, the said heat flux was adjusted through 24 hours taking into account the effect from the neighboring casks stored every three meters at the site and leaving 400 W/m^2 to the concrete cover under normal conditions and 100 W/m^2 to the cylinder. The outer bottom surface of the SNF cask was assumed to receive no solar flux. No heat radiation as considered from the cylinder of the cask as the neighboring casks has similar temperatures.

The analysis performed covered three stages of thermal accidents: before fire (steady-state conditions), fire (transient conditions), and post-fire stage (transient conditions). In order to identify the distribution of the temperature in the cask, a steady-state analysis was carried out. The obtained information was applied as input data to the models of transient fire and post-fire stage. The convective heat transfer coefficient for laminar flow of 5 W/m^{2}K indicated on the outer cask surface was applied for the evaluation of heat transfer between the cask and the surroundings.

Once a stable solution was achieved, transient calculations were made for fire accident modeling. As it has been mentioned above, a transportation cask is designed to sustain the temperature of 800 °C for 30 minutes or 600 °C for 60 minutes [7,32] in the case of an accident and remain undamaged. In this study, both conditions were modeled for a storage cask. In the IAEA requirements [7] it is

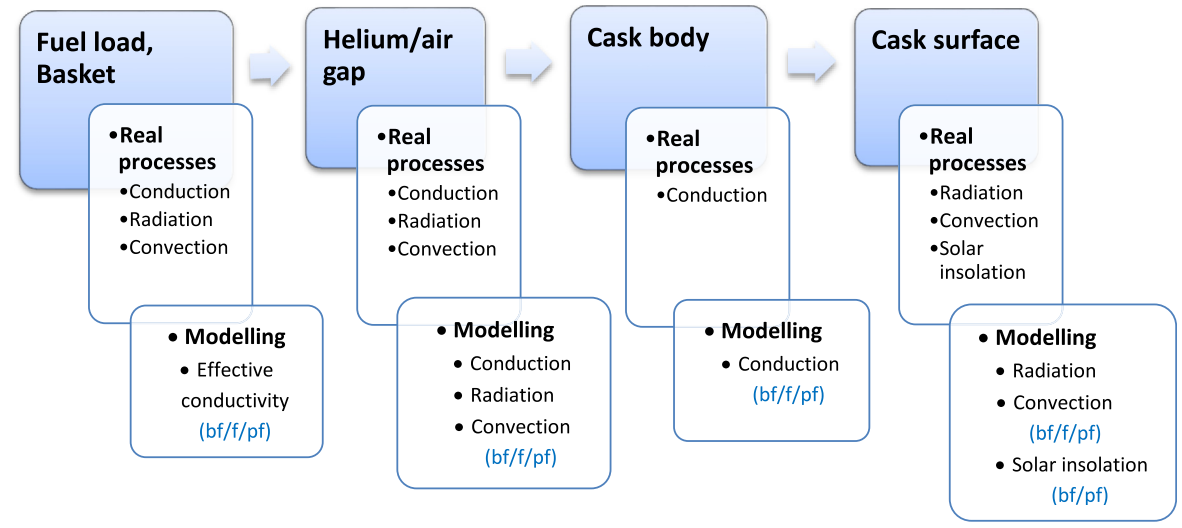

Fig. 2. Thermal processes in the cask and assumptions for modeling.

indicated that the average flame emissivity coefficient of 0.9 is applied to a model representing a cask affected by thermal conditions. However, as the study of [33] showed, the coefficient is 1.0 when the flame intensifies (for example, hydrocarbon flames). Thus, the present study also applied the higher coefficient. The internal cask elements would heat up because of the radiative heat flux affecting the cask walls. The applied absorption coefficient for all surfaces in the case of fire was 1. The internal heat generation because of radioactive decay was assumed to be the same as in normal conditions. Solar insolation was not assessed in the modeling of fire.

As in the previous study [25], it was assumed that the convective heat transfer coefficient for the outer surface during fire is 15 W/m^{2}K.

During the post-fire stage, the heat gained during the fire slowly dissipates from the cask outer surfaces. During this stage, the usual cooling of the basket is more complicated, and thus, the temperature of the basket rises. The numerical modeling was carried out until the central zone of the basket reached the maximum temperature and began to decrease. The internal heat generation because of radioactive decay was the same as in normal conditions. For the post-fire stage, the emissivity coefficient was assumed to be 0.93 and the ambient temperature 37 °C, and the solar heat flux was taken into account. Also, the coefficient of convective heat transfer for laminar flow was assumed to be 5 W/m^{2}K on the outer cask surfaces.

The thermal state of the SNF cask was analyzed using the ANSYS Fluent code, which solves heat transfer processes in complex geometries. For the modeling of heat transfer in the helium gap and air gaps, transient equations were applied for the fire and post-fire stages. For the stage before fire, steady-state Navier-Stokes equations for laminar flow were used.

The Discrete Ordinates (DO) method [34] implemented in the ANSYS Fluent code was employed for radiation in the helium gap and air gaps. This method discretizes radiative transport equations into a finite number of solid angles and solves the equations on the same finite volume mesh as the flow and convective heat transfer equations, coupled through appropriate source terms.

Boundary conditions on the cask outer surface are set as in [25].

As the cask is symmetrical and there appear to be no significant variations of heat transfer around its perimeter, a 2D model of a symmetrical cask was employed. All elements of the cask were represented as separate zones (Fig. 1). Higher resolution of the mesh is created in the zones of the helium gap and the air gap between the cask lid and the guard plate. Three different meshes (170400, 278000 and 620700 elements) were tested in order to learn if the number of mesh elements influences the results of the analysis. Mesh validation results and Grid Convergence Index (GCI) [35], calculated in respect to fine grid, for steady-state and transient fire conditions are presented in Table 1. As Table 1 demonstrates, all three cases show small difference in the temperatures. Hence, the mesh with 278 thousand hexahedral elements was used for the modeling.

The mesh control parameters were tuned in ANSYS Workbench Meshing module and it created the mesh.

Convergence criteria were used for the determination of the numerical simulation's convergence to a solution that is when the solution residual values do not exceed the following magnitudes: 10^{-3} for continuity and momentum equations, 10^{-6} for energy and radiation equations.

3. Results

As it has been indicated above, the object of the thermal analysis performed was the cask in an open storage facility with extreme summer conditions: exposed to solar insolation and 37 °C of the ambient temperature. The results obtained during the analysis were accepted as starting conditions for the thermal analysis of a fire accident. During the modeling of the fire accident, the ambient temperature was kept constant and was 800 °C for the duration of 30 minutes and 600 °C for the duration of 60 minutes. Finally, a thermal analysis of post–fire conditions was performed. All the modeled cases are presented in Fig. 3 and Table 2.

Fig. 3a shows the temperature distribution before the fire accident. The maximum temperature is in the center of the fuel load. The temperature gradually decreases receding from the center in radial as well as in axial directions. The cask body temperature in axial direction varies similarly. The maximal temperatures of the inner surface of the cask body (1), of the protective cover (7) and of the cask's bottom are also in the center. The corners of the body and

Table 1
Mesh validation.

Mesh	Element count	Max temperature (fuel load) at steady-state condition	GCI at steady-state condition	Max temperature (outer surface) after 30 min 800°C fire	GCI after 30 min 800°C fire	Max temperature (outer surface) after 60 min 600°C fire	GCI after 60 min 600°C fire
Coarse	170400	252.689	0.0003	701.693	0.003	532.512	0.003
Normal	278000	252.667	0.0004	703.171	0.001	533.808	0.003
Fine	620700	252.657		703.523		533.183	

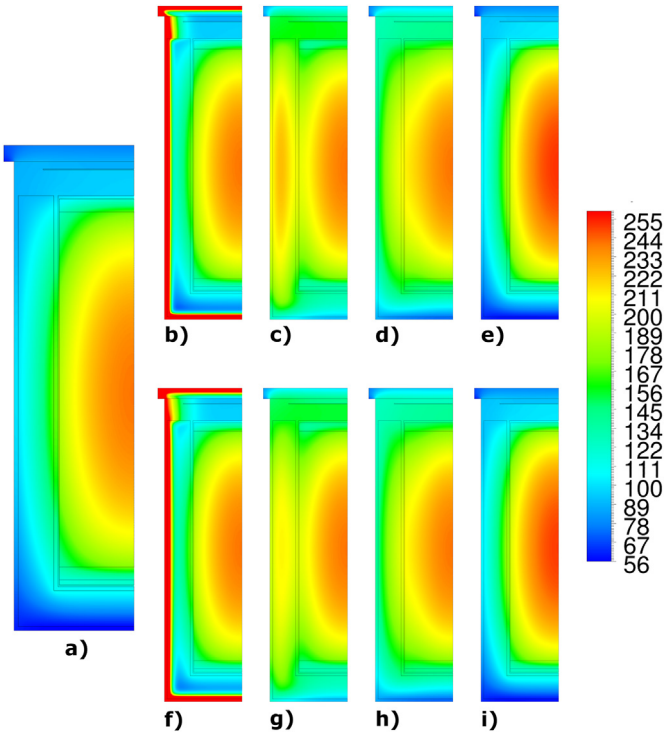

Fig. 3. Cask temperature distribution: a) before the fire, b) just after the 30 min. 800 °C fire, c) 11 h after the onset of the fire (800 °C for 30 min), d) 24 h after the onset of the fire (800 °C for 30 min), e) 6 days after the onset of the fire (800 °C for 30 min), f) just after the 60 min. 600 °C fire, g) 11 h after the onset of the fire (600 °C for 60 min), h) 24 h after the onset of the fire (600 °C for 60 min), i) 6 days after the onset of the fire (600 °C for 60 min).

the bottom part close to the ground have the lowest temperatures.

Since the temperature scale in case of fire is different (higher temperature) than temperatures after the fire, the results are presented in the same temperature scale as for steady-state conditions in order to highlight the parts of the cask that heat up during fire. The actual modelled maximum temperature during a fire is about 700 °C.

Fig. 3b shows the temperature distribution inside the cask just after the fire accident that lasted for 30 minutes and sustained the constant temperature of 800 °C. At this moment, the outer surface (3) of the cask has the highest temperature. Due to the concrete cover (7), low heat conductivity and large heat capacity heat transfer through the concrete cover (7) into the internal layers of the cask body are quite slow. The cask body (1) is made from heavy concrete but it is still rather high resistance for heat transfer to the fuel load. The metal linings (2, 3) of the cask body practically do not create resistance for heat transfer.

Fig. 3c, d, e show the temperature distribution for post–fire conditions. The heat accumulated in the cask body during the fire accident slowly dissipates to the inner parts of the cask and the external environment. After 11 hours (Fig. 3c), the cask body (1) temperature is still rather high but has decreased significantly, and the highest temperature of the cask is already in the center of the fuel load as before the fire accident (Fig. 3a). The bottom of the cask and the top of the concrete cover (7) has much lower temperatures compared to the temperature of the cask's outer surface (3) on the side wall. After 24 hours (Fig. 3c), the temperature of the cask body (1) has decreased, and the highest temperature of the cask is in the center of the fuel load. After 6 days (Fig. 3d), the temperature distribution is similar to that before the fire accident (Fig. 3a).

In the case of a 60 min. 600 °C fire accident (Fig. 3f), the temperature distribution is very similar to the case of the 30 min. 800 °C fire accident. However, due to longer fire duration, the top and bottom parts of the container are hotter. The opposite situation is observed for post-fire conditions at (11 h) where the cask body (1) temperature is lower (Fig. 3g) in comparison to the 30 min. 800 °C fire accident (Fig. 3c). As the cask body (1) overheats less, the fuel load receives less additional heat (Fig. 3i).

Fig. 4 shows the comparison of the radial temperature distribution before the fire accident, just after the fire, 11 h, 24 h and 6 days from the moment when the fire has started. The temperatures in Fig. 4 are limited to 300 °C. This yields a cut of curves which represents the outer surface temperatures with max 700 °C at the end of the fire (Fig. 4a) and 540 °C (Fig. 4b).

As Fig. 4a shows, in the case where fire lasts for 30 minutes and its temperature is 800 °C, the maximum temperature of the cask before the fire is about 247 °C and is in the center ($r/r_0 = 0$) of the fuel load and decreases gradually through the fuel load ($r/r_0 = 0$ - 0.63). Then there is a rather sharp temperature drop through the

Table 2
Cask temperature distribution for different modelled cases.

Fig. 3 letters	Condition		
	No fire	Fire (800 °C for the duration of 30 minutes)	Fire (600 °C for the duration of 60 minutes)
A	before the fire		
b		just after the fire	
c		post–fire conditions (after 11 hours)	
d		post–fire conditions (after 24 hours)	
e		post–fire conditions (after 6 days)	
f			just after the fire
g			post–fire conditions (after 11 hours)
h			post–fire conditions (after 24 hours)
i			post–fire conditions (after 6 days)

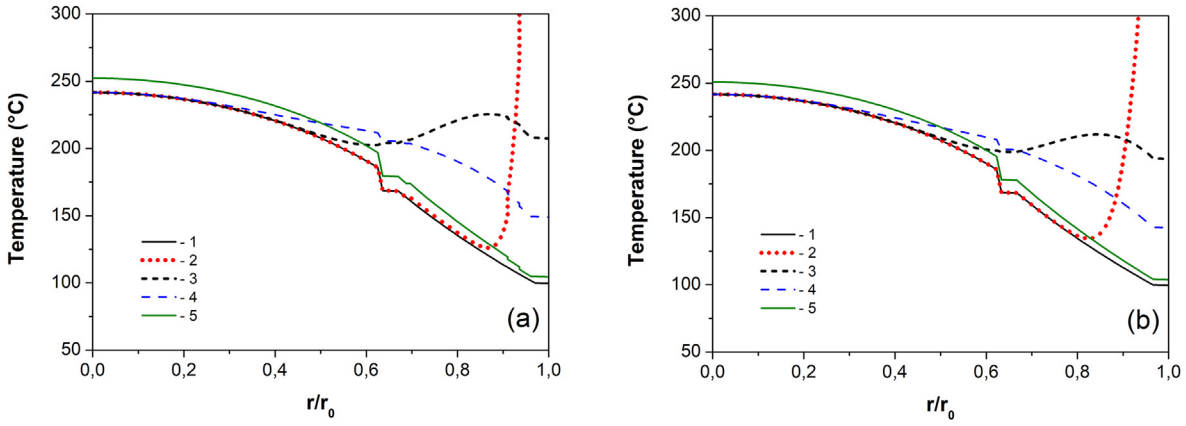

Fig. 4. The comparison of the radial temperature distribution in the middle of the cask for a) 30 minute fire at 800 °C and for b) 60 minute fire at 600 °C at different fire periods: 1) before the fire, 2) just after the fire, 3) 11 hours after the onset of the fire, 4) 24 hours after the onset of the fire, 5) 6 days after the onset of the fire.

helium gap ($r/r_0 = 0.63$ - 0.65). In the inner metal lining ($r/r_0 = 0.65$ - 0.68), the temperature drop is insignificant because of the good thermal conductivity of the lining. Heavy concrete ($r/r_0 = 0.68$ - 0.97) has significant thermal resistance, and therefore, the temperature drop through it is significant. The temperature drop, through the outer metallic lining ($r/r_0 = 0.98$ - 1) is also insignificant.

During the 30 minute fire, the temperature of the outer surface increased significantly as well and, as it has already been indicated above, reached 700 °C. However, because of the rather high thermal resistance of the heavy concrete, the outer surface's temperature increased only in about one third of the surface thickness ($r/r_0 \sim 0.9$ - 0.94) and in the remaining part of the surface, including fuel load, remained at the temperature that was before the fire.

After the fire, the temperature of the outer surface decreased rather quickly and after 11 and 24 hours from the beginning of the fire it was about 200 °C and 150 °C respectively. During these time periods, the temperature increased towards the center of the cask, i.e. till $r/r_0 \sim 0.5$ and $r/r_0 \sim 0.3$ respectively, with the maximum unchanged temperature still remaining in the center of the fuel load.

Six days after the fire, the temperature of the cask outer surface was close to the temperature before the fire. However, the fuel load temperature increased and its maximum in the center of the fuel load was about 252 °C.

In the case of the 60 minute fire at 600 °C (Fig. 4b), radial temperature distributions were similar to the previous case (Fig. 4a). With time the temperature increase shifted to the center of the cask.

Fig. 5 shows a direct comparison of the temperature variations at different times for both cases analyzed. In the case of the 30 minute fire at 800 °C (Fig. 5a), the maximum temperature of 700 °C at the end of the fire decreases rapidly and after about 11 hours is equal to the maximum load temperature in the center of the cask. In the case of the 60 minute fire at 600 °C, the temperature of the cask outer surface is lower, and only at the end of the fire it exceeds a little the post fire temperature of the 30 minute fire at 800 °C. However, a significant difference between the maximum temperatures is observed at the end of the fires, i.e., 700 °C for the fire of longer duration and 540 °C for the fire of shorter duration. After about 11 hours from the beginning of fire, in both cases these temperatures are very similar.

Fig. 5b demonstrates a comparison of the temperature variations with time in the center of the cask. For both cases, after 24 hours from the beginning of the fire the temperature in the center of the cask starts to increase. The max temperature is reached after 125 h (5 days), and after that it gradually decreases. The maximum increase in the temperatures as a result of fire is about 10 °C and 8 °C for the 30 minute fire at 800 °C and for the 60 minute fire at 600 °C, respectively.

As it has been indicated above (Fig. 4), it is a rather sharp temperature drop through the helium gap. The variations of this temperature drop are presented in Fig. 6. The figure shows that before fire at steady-state conditions the temperature difference between the higher basket surface temperature and the lower metallic lining inner surface temperature is about 17 °C. During the post fire period, the lining temperature increases and therefore the temperature difference decreases and reaches the minimum after about 11 hours from the beginning of the fire. For the case of the 60 minute fire at 600 °C, the difference in the temperature is nearly zero. For the case of the 30 minute fire at 800 °C, the difference in the temperature becomes negative, i.e., the temperature of the metallic lining inner surface is slightly higher than the temperature of the basket outer surface. Such variation in the temperature difference through the helium gap has impact on the flow hydrodynamics in this gap.

4. Sensitivity analysis

The impact that the parameter uncertainties could have on the cask temperatures was evaluated through local sensitivity analysis. The following are the selected parameters with their justification:

- *Decay heat of SNF* depends on, for example, fuel enrichment, the positioning in the reactor during its operation, fuel enrichment.
- *Effective thermal conductivity coefficient of fuel load* is an experimentally defined value with uncertainties.
- *Temperature of fire* is not strongly defined because the value may vary according to intensity and sources of fire.
- *Duration of the fire accident* depends on the source of fire and the response produced by people.

Other uncertainties include solar insolation, ambient temperature, and the impact from adjacent casks on the ambient

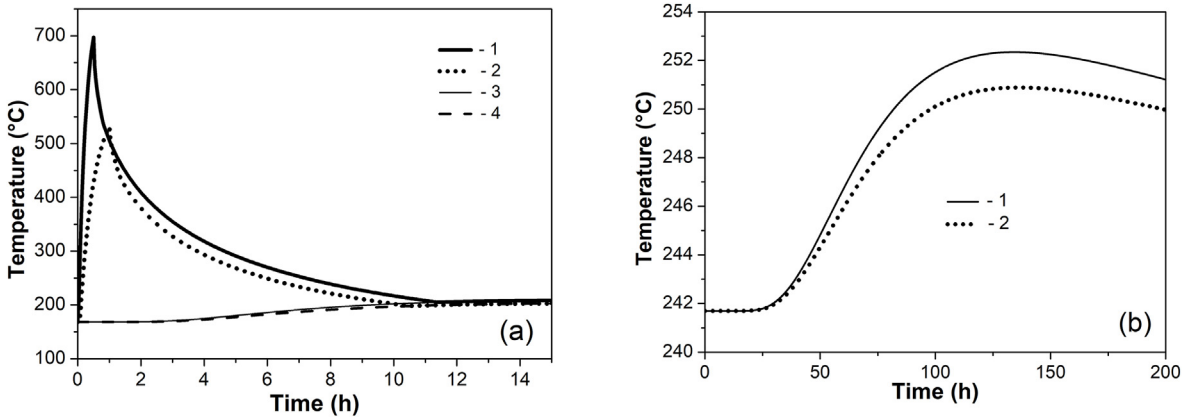

Fig. 5. Comparison of the temperature variations on the outer surface (a): 1 - outer surface of the cask body 30 min 800 °C fire, 2 - outer surface of the cask body 60 min 600 °C fire, 3 - inner surface of the cask body 30 min 800 °C fire, 4 - inner surface of the cask body 60 min 600 °C fire; and in the center of the cask (b): 1–30 min 800 °C fire; 2–60 min 600 °C fire.

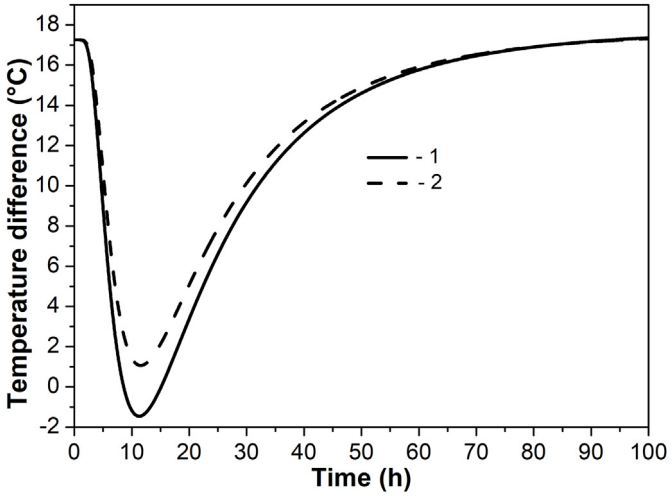

Fig. 6. Variation in the temperature difference through the helium gap with time: 1–30 min 800 °C fire; 2–60 min 600 °C fire.

temperature. These uncertain parameters are certainly impactful under steady-state conditions. However, their impact during fire is negligible, and thus this sensitivity analysis did not consider these parameters.

Possible deviations by ±20% of the parameters were assumed. The results of the investigation of the influence of the parameters on maximum temperatures of the fuel load are shown in Fig. 7.

The temperature distribution under steady–state conditions is affected by the effective thermal conductivity coefficient of fuel load and the decay heat of the spent nuclear fuel. Fig. 7 presents the quantitative evaluation of the deviation from the initial temperature. As the diagram shows the decay heat exerts the impact of up to 12 percent on the maximum fuel load temperature, while the impact of basket conductivity is twice lower.

The fuel load is quite inertial and thus, as it has been demonstrated above, the fuel load temperature during the fire remains unchanged and changes slowly after the fire accident. Six days after the fire the temperature of the fuel load reaches its maximum. The uncertainty was evaluated as well, since the temperature was also affected by uncertainty parameters (Fig. 7b). As Fig. 7 shows, the fuel load conductivity and the decay heat have the strongest impact: up to 11 percent, while the impact of the fire temperature is less than three percent and of the fire duration about one percent.

The maximum basket temperature is compared to the corresponding temperature in the base solution. The evaluated deviation is presented in Fig. 7c. As the figure shows, the decay heat exerts the impact of 12 percent, while the impact of the fuel load conductivity is twice as low, i.e., up to six percent. Then the deviation is also caused by the fire temperature uncertainty (the impact of up to two percent) and the accident time (the impact of up to one percent).

5. Conclusions

The analysis of the thermal state of the CONSTOR RBMK-1500 cask under the simulated conditions yielded the following findings:

1. During the fire, only the outer parts of the cask body are heated, and the heat accumulated in those parts heats the fuel load as well as dissipates to the ambient air in the post-fire period.
2. Under steady-state conditions, the temperature drop through the vertical helium gap is about 17 °C. During the fire it does not change. However, in the post-fire period the temperature decreases and 11 hours after the fire it is close to zero. After that this temperature drop recovers with time.
3. The maximum temperature of the fuel load does not change during the fire. However, it increases during the post–fire period and reaches its maximum 6 days after the end of the fire.
4. The maximum increase in the temperatures as a result of the fire is about 10 °C and 8 °C for the 30 minute fire at 800 °C and the 60 minute fire at 600 °C respectively.
5. During the fire and the post–fire period, the fuel load temperatures did not exceed the 300 °C limiting temperature set for an RBMK SNF cladding for long–term storage in an inert nitrogen or helium environment (normal conditions). This means that a fire accident cannot cause overheating of the fuel rods in a cask.
6. The local sensitivity analysis revealed that the uncertainties of the decay heat and the effective conductivity of the fuel load have the highest impact on the maximum temperatures of the fuel load.

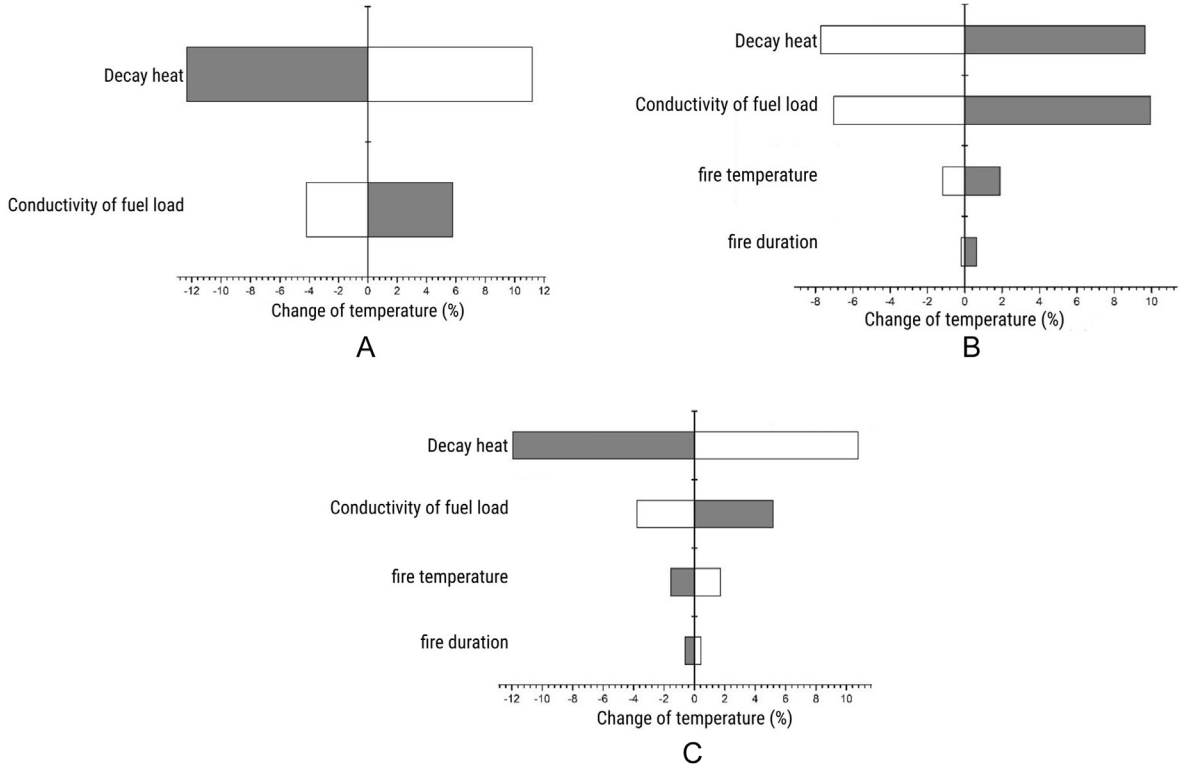

Fig. 7. Sensitivity assessment for 30 min 800 ^{o}C fire: a) – maximum fuel load temperature before fire, b) – time to reach maximal fuel load temperature, c) – maximum fuel load temperature for post fire. White color indicates enlarged parameters; grey color indicates reduced parameters.

Declaration of competing interest

The authors declare that they have no known competing financial interests or personal relationships that could have appeared to influence the work reported in this paper.

References

[1] M. Wataru, H. Takeda, K. Shirai, T. Saegusa, Thermal hydraulic analysis compared with tests of full-scale concrete casks, Nucl. Eng. Des. 238 (2008) 1213–1219, https://doi.org/10.1016/j.nucengdes.2007.03.036.
[2] L.E. Herranz, J. Penalva, F. Feria, CFD analysis of a cask for spent fuel dry storage: model fundamentals and sensitivity studies, Ann. Nucl. Ener. 76 (2015) 54–62, https://doi.org/10.1016/j.anucene.2014.09.032.
[3] Y.S. Jeong, I.C. Bang, Hybrid heat pipe based passive cooling device for spent nuclear fuel dry storage cask, App. Therm. Eng. 96 (2016) 277–285, https://doi.org/10.1016/j.applthermaleng.2015.11.086.
[4] M.G. El-Samrah, A.F. Tawfic, S.E. Chidiac, Spent nuclear fuel interim dry storage: design requirements, most common methods, and evolution: a review, Ann. Nucl. Energy 160 (2021), 108408, https://doi.org/10.1016/j.anucene.2021.108408.
[5] S. Alyokhina, A. Kostikov, Unsteady heat exchange at the dry spent nuclear fuel storage, Nucl. Eng. Technol. 49 (2017) 1457–1462, https://doi.org/10.1016/j.net.2017.07.029.
[6] M. Hanifehzadeh, B. Gencturk, R. Mousavi, A numerical study of spent nuclear fuel dry storage systems under extreme impact loading, Eng. Struct. 161 (2018) 68–81, https://doi.org/10.1016/j.engstruct.2018.01.068.
[7] IAEA Safety Standards SeriesNo, SSR-6 (Rev.1), Regulations for the safe transport of radioactive, Mat. Specif. Saf. Require. (2018) 165.
[8] K.S. Bang, S.H. Yu, J.C. Lee, K.S. Seo, W.S. Choi, Experimental assessment on the thermal effects of the neutron shielding and heat-transfer fin of dual purpose casks on open pool fire, Nucl. Eng. Des. 304 (2016) 63–69, https://doi.org/10.1016/j.nucengdes.2016.04.040.
[9] R.L. Frano, G. Pugliese, G. Forasassi, Thermal analysis of a spent fuel cask in different transport conditions, Energy 36 (2011) 2285–2293, https://doi.org/10.1016/j.energy.2010.01.041.
[10] Y.S. Tseng, J.R. Wang, F.P. Tsai, Y.H. Cheng, C. Shih, Thermal design investigation of a new tube-type dry-storage system through CFD simulations, Ann. Nucl. Energy 38 (2011) 1088–1097, https://doi.org/10.1016/j.anucene.2011.01.001.
[11] J. Li, Y.Y. Liu, Thermal modelling of a vertical dry storage cask for used nuclear fuel, Nucl. Eng. Des. 301 (2016) 74–88, https://doi.org/10.1016/j.nucengdes.2016.01.008.
[12] J. Benavides, G. Jimenez, M. Galban, M. Lloret, Methodology for thermal analysis of spent nuclear fuel dry cask using CFD codes, Ann. Nucl. Energy 133 (2019) 257–274, https://doi.org/10.1016/j.anucene.2019.05.026.
[13] S.H. Yoo, H.C. No, H.M. Kim, E.H. Lee, Full-scope simulation of a dry storage cask using computational fluid dynamics, Nucl. Eng. Des. 240 (2010) 4111–4122, https://doi.org/10.1016/j.nucengdes.2010.08.009.
[14] J.M. Creeret, et al., The TN-24P PWR spent fuel storage cask: testing and analysis, in: EPRI NP-5128, PNL-6054, Pacific Northwest Laboratory, 1987.
[15] R.A. Brewster, E. Baglietto, E. Volpenhein, C.S. Bajwa, CFD analyses of the TN-24p PWR spent fuel storage cask, in: The ASME 2012 Pressure Vessels & Piping Division Conference, 2012, https://doi.org/10.1115/PVP2012-78491. Paper No.PVP2012-78491, Toronto, USA, July 15–17.
[16] P. Poškas, A. Šmaižys, V. Šimonis, Radiological and thermal characteristics of CASTOR RBMK-1500 and CONSTOR RBMK-1500 casks for spent nuclear fuel storage at ignalina nuclear power plant, Kerntechnik 71 (2006) 222–227, https://doi.org/10.3139/124.100297.
[17] R. Poškas, V. Šimonis, P. Poškas, A. Sirvydas, Thermal analysis of CASTOR RBMK-1500 casks during long-term storage of spent nuclear fuel, Ann. Nucl. Energy 99 (2017) 40–46, https://doi.org/10.1016/j.anucene.2016.09.031.
[18] Ye.T. Koyanbayev, M.K. Skakov, D.A. Ganovichev, Ye.A. Martynenko, A.A. Sitnikov, Simulation of the thermal conditions of cask with fuel assemblies of BN-350 reactor for dry storage, Sci. Technol. Nucl. Install. vol. 2019 (2019) Article ID 3045897, 5 pages, doi:10.1155/2019/3045897.
[19] W.J. Cho, S. Kwon, K.S. Kim, Rock cavern storage of spent fuel, J. Nucl. Fuel Cycle Waste Technol. 13 (2015) 301–313, https://doi.org/10.7733/jnfcwt.2015.13.4.301.
[20] S.H.A. Latif, M.M. Kandil, A.M. Refaey, S.A. Elnaggar, Simulation of partial and complete loss of flow accidents for GPWR using ATHLET code, Int. J. Thermofluids 11 (2021), 100097, https://doi.org/10.1016/j.ijft.2021.100097.
[21] B. Almomania, D. Janga, S. Leeb, H.G. Kang, Development of a probabilistic safety assessment framework for an interim dry storage facility subjected to

an aircraft crash using best-estimate structural analysis, Nucl. Eng. Technol. 49 (2017) 411–425, https://doi.org/10.1016/j.net.2016.12.013.
[22] C.S. Bajwa, An Analysis of a Spent Fuel Transportation Cask under Severe Fire Accident Conditions, 2002. Technical Report, https://www.nrc.gov/docs/ML0216/ML021690443.pdf.
[23] D. Sanyal, P. Goyal, V. Verma, A. Chakraborty, A CFD analysis of thermal behaviour of transportation cask under fire test conditions, Nucl. Eng. Des. 241 (2011) 3178–3189, https://doi.org/10.1016/j.nucengdes.2011.06.017.
[24] P. Geraldini, A. Lorenzo, Numerical Analysis and Experimental Verification of a Fire Resistant Overpack for Nuclear Waste, Proc. 2016 COMSOL Conference, Munich, Germany, 2016.
[25] R. Poškas, P. Poškas, K. Račkaitis, R. Zujus, A numerical study of thermal behavior of CASTOR RBMK-1500 cask under fire conditions, Nucl. Eng. Des. 376 (2021), 111131, https://doi.org/10.1016/j.nucengdes.2021.111131.
[26] R. Poškas, V. Šimonis, H. Jouhara, P. Poškas, Modeling of decay heat removal from CONSTOR RBMK-1500 casks during long-term storage of spent nuclear fuel, Energy 170 (2019) 978–985, https://doi.org/10.1016/j.energy.2018.12.217.
[27] J.C. Lee, W.S. Choi, K.S. Bang, K.S. Seo, S.Y. Yoo, Thermal-fluid flow analysis and demonstration test of a spent fuel storage system, Nucl. Eng. Des. 239 (2009) 551–558, https://doi.org/10.1016/j.nucengdes.2008.12.015.
[28] A.V. Vatulin, A.G. Ioltukhovskiy, I.M. Kadarmetov, et al., Validation of dry storage modes for RBMK-1000 spent fuel assembles (SFA) (IAEA-CN-102/39), in: Storage of Spent Fuel from Power Reactors. Proceedings of International Conference, IAEA, Vienna, Austria, 2003, pp. 422–430.
[29] V.I. Kalinkin, V.G. Kritskij, N.N. Davidenko, et al., Technology of SNF RBMK1500 Transfer from "Wet" to "Dry" Storage, JSC Head Institute VNIPIET and JSC Concern Rosenergoatom, St. Petersburg, Russia, 2010.
[30] J.C. Lee, K.S. Bang, K.S. Seo, H.D. Kim, B.I. Choi, H.Y. Lee, Thermal analysis of a spent fuel storage cask under normal and off-normal conditions, J. Korean Rad. Waste Soc. 2 (2004) 13–22.
[31] E. Bich, J. Milat, E. Vogel, The viscosity and thermal conductivity of pure monatomic gases from their normal boiling point up to 5000 K in the limit of zero density and at 0.101325 MPa, J. Phys. Chem. Ref. Data 19 (1990) 1289–1305.
[32] M.D. Valkeneer, Spent Fuel Management in Belgium, 1995. Proc. of IAEA-NEA Symposium Safety and Engineering Aspects of Spent Fuel Storage. IAEA-SM-335/3.
[33] D. Dougal, An Introduction to Fire Dynamics, third ed., Wiley., 2011.
[34] J.Y. Murthy, S.R. Mathur, Finite volume method for radiative heat transfer using unstructured meshes, J. Thermophys. Heat Trans. 12 (1998) 313–321.
[35] P.J. Roache, Quantification of uncertainty in computational fluid dynamics, Annu. Rev. Fluid Mech. 29 (1997) 123–160.